Materials Chemistry and Physics 133 (2012) 259–262

Contents lists available at SciVerse ScienceDirect

Materials Chemistry and Physics

journal homepage: www.elsevier.com/locate/matchemphys

Electrically controlling infiltration pressure in nanopores of a hexagonal mesoporous silica

Weiyi Lu [a], Taewan Kim [b], Aijie Han [c], Yu Qiao [a,b,*]

[a] Department of Structural Engineering, University of California – San Diego, La Jolla, CA 92093-0085, United States
[b] Program of Materials Science & Engineering, University of California – San Diego, La Jolla, CA 92093, United States
[c] Department of Chemistry, University of Texas – Pan American, Edinburg, TX 78539, United States

ARTICLE INFO

Article history:
Received 24 May 2011
Received in revised form 5 January 2012
Accepted 7 January 2012

Keywords:
Nanopores
HMS
Electric field
Infiltration

ABSTRACT

With the addition of copper microparticles, the electrical conductivity of a hexagonal mesoporous silica (HMS) disk can be enhanced. As an electric field is applied across the interface of the HMS–Cu mixture and an electrolyte solution, the liquid infiltration pressure increases considerably, which is also dependent on the nanopore size. It may be attributed to the surface charge effect, which is amplified by the large surface to volume ratio.

1. Introduction

Understanding fluidic behaviors on nanoscale is critical to a variety of applications, e.g. [1,2]. Nanofluidic behaviors are fundamentally different from the predictions of continuum theory. At the molecular level, as water molecules are confined in a nanopore, their configuration is strongly affected by the solid atoms. Along the axial direction, because the pore depth is much longer than the characteristic diffusion distance, the liquid structure is quite uniform [3]. Along the radius direction, the confined liquid molecules may form a few layers, depending on the surface features [4]. If there are solvated ions, the system may become heterogeneous [5,6]. In a molecular sized nanopore, the ions cannot be fully solvated, and they may form crystalline-like clusters [7,8]. If the nanopore is relatively large, the hydration shell may be formed but are distorted [9]. The coordination number tends to decrease, and the structure can be anisotropic.

As a pressure gradient exists, water molecules and ions would move from the high potential area to the low potential area. If the nanopore is short, the molecules can rapidly transport across it in a "frictionless" manner [10]. In a long nanopore, the "column resistance" offered by the solid atoms must be taken into consideration, and a number of fundamental properties of the confined liquid, including the effective viscosity and the effective surface tension, must be re-investigated [11,12].

Other than external pressure, confined liquids would also respond to thermal and electric fields. When temperature changes, the effective solid–liquid interfacial tension in nanopores can vary considerably, somewhat similar to the classic thermocapillary effect [13]. The excess interfacial tension can trigger a net motion of liquid molecules, either into or out of the nanopores. Previous experimental results also showed that the liquid transport pressure in nanopores can be adjusted by a voltage [14,15]. In order to separate the nanoporous electrode and the confined liquid, the nanopore inner surfaces were coated by a monolayer of field responsive groups. Thus, as the molecular configurations change with the potential difference, the effective interfacial tension varies, affecting the ion transport behaviors. A nonconductive nanoporous phase can be employed as the insulation layer [16]. Note that, in such a setup, the applied voltage must be high, at the level of 10^2 V, comparable with the voltage in a classic electrowetting test on a large, flat surface.

Many nanoporous materials, such as silica, are nonconductive. To extend their applications to electrowetting study, their conductivity should be improved, e.g. through addition of a conductive phase. Similar methods have been used to form nanoporous electrodes in energy conversion systems [17]. The influence of the secondary, conductive phase on the nanofludic behaviors is still inadequately understood.

* Corresponding author at: Department of Structural Engineering, University of California – San Diego, La Jolla, CA 92093-0085, United States. Tel.: +1 858 534 3388; fax: +1 858 534 1310.
E-mail address: yqiao@ucsd.edu (Y. Qiao).

0254-0584/$ – see front matter © 2012 Elsevier B.V. All rights reserved.
doi:10.1016/j.matchemphys.2012.01.019

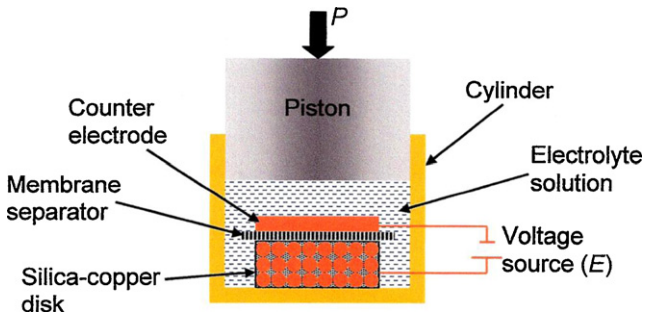

Fig. 1. Schematic of the experimental setup.

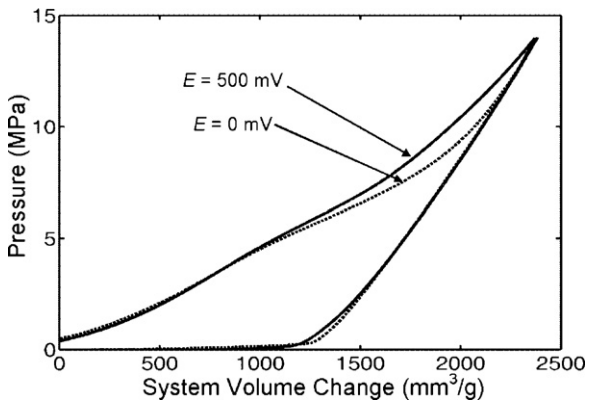

Fig. 2. Typical sorption isotherm curves.

2. Experimental

The nanoporous material analyzed in the current investigation was a Sigma–Aldrich hexagonal mesoporous silica (HMS). It was a nonconductive powder material, with the particle size around a few to tens of μm. To directly measure the ion transport pressure, it was surface treated. The material was dehydrated in vacuum at 100 °C for 12 h. At 90 °C, 1 g of HMS was mixed with 40 ml of dry toluene and 1 ml of chlorotrimethylsilane. The mixture was vigorously stirred for 36 h, after which the HMS sample was filtered, dehydrated in vacuum at 120 °C for 12 h, and rinsed repeatedly with methanol and dry toluene. According to a Barret–Joyner–Halenda (BJH) measurement, the nanopore size was mostly in the range of 2–7 nm and the modal value was around 3 nm.

The treated HMS was uniformly mixed with Dendritic-3 μm copper (Cu) microparticles, with the silica–copper ratio of 1:1.5. The average size of the copper particles was 3 μm. The HMS–Cu mixture was compressed into thin disks under 10 MPa, with the disk thickness around 460 μm. Note that the silica nanoporous structure could remain stable up to a few hundreds MPa [18], much higher than the pressure range involved in the current study.

A HMS–Cu disk was placed in a stainless steel cylinder, as depicted in Fig. 1, separated from a gold counter electrode by a 250 μm thick porous polypropylene membrane. The electrodes were immersed in a 15% aqueous solution of lithium chloride (LiCl). Across the HMS–Cu disk and the counter electrode, a voltage, $E = 0.5$ V, was applied. The cylinder was sealed by two stainless steel pistons with reinforced gaskets. In a type 5580 Instron machine, the upper piston was intruded into the cylinder at the rate of 1 mm min^{-1}. The piston pressure and the piston displacement were measured continuously. Once the pressure reached about 14 MPa, the piston was moved out at the same rate.

3. Results and discussion

Typical sorption isotherm curves are shown in Fig. 2. After the surface treatment, the nanopore walls are coated by hydrophobic silyl groups and become nonwettable to the liquid phase [19]. The sorption isotherm curve consists of a few stages. The dashed line indicates the system behavior when $E = 0$ V. The low-pressure section from 0 MPa to about 4 MPa is quite linear. When the pressure rises, the system volume is reduced smoothly, reflecting the linear compression of the liquid phase and the machine compliance. From about 4 MPa, the sorption isotherm curve becomes nonlinear. Since both the HMS and the liquid phases are incompressible in this pressure range, the formation of the plateau must be attributed to the pressure induced infiltration. At the relatively high pressure, the bulk liquid phase can overcome the repelling effect of the nanopore walls, and the liquid starts to enter into the nanoporous space. The liquid infiltration starts with the relatively large nanopores. As pressure increases, smaller nanopores are filled. When the pressure reaches about 8 MPa, the slope of sorption isotherm curve becomes linear again and increases rapidly, converging to the bulk modulus of the liquid phase, indicating that the nanoporous space is occupied and no more liquid infiltration would occur. Note that the width of the infiltration plateau is close to the BJH measurement result of nanopore volume.

As the pressure further increases, the nominal system volume change is determined by the compressibility of the liquid phase as well as the compliance of the testing machine. These factors are independent of the HMS properties, and are not affected by the external electric field.

Upon unloading, the system volume does not recover, suggesting that the confined liquid does not defiltrate. The irreversibility of liquid infiltration and defiltration may be related to the energy barrier of nanopore walls to the liquid motion [20], i.e. the "column resistance" [21]. It may also be caused by the "blocking effect" of confined gas/vapor nanophases, which has unique characteristics as the effective solubility is reduced by the nanopore surfaces [22]. The details of liquid defiltration are still under investigation. The following discussion will be focused on the liquid infiltration phenomena.

The copper and the HMS particles can be mixed together quite uniformly. The former can form a semi-continuous, conductive matrix. When it is connected to the voltage source, the surface of the copper particles would be of a higher potential than the liquid phase. In the framework of conventional electrowetting theory, at a large solid surface, there is a high-ion-density interface double layer, which can sometimes be modeled as the Outer Helmholtz Plane (OHP) [23]. The molecular structure and the ion density in OHP determine the effective solid–liquid interfacial tension. When an electrical potential difference is created, according to the classic Lippmann equation, the interfacial tension tends to decrease [24]. Therefore, the capillary pressure that a liquid must overcome to enter a pore should be reduced. If the solid surface is conductive, the interfacial tension change can occur at a low voltage. If the electrode is coated with a monolayer of surface groups, the nonconductive coating promotes the capacitive effect and suppresses current formation, so that larger contact angle changes may be achieved at similar voltages [25–27]. With an insulation layer of the thickness at the level of $10–10^2$ μm, the required voltage is typically tens to a few hundreds volts; otherwise the contact angle variation would be negligible [24].

The liquid infiltration takes place in the nanopores of HMS. The silyl monolayer is coated on the nonconductive silica. This is fundamentally different from the experiments on monolayer coated large metallic electrodes [25–27], where the insulation layers contained only the surface groups. In the current investigation, the conductive phase (Cu) and the liquid phase are separated by the silica network. The silica particle size is as large as tens of microns.

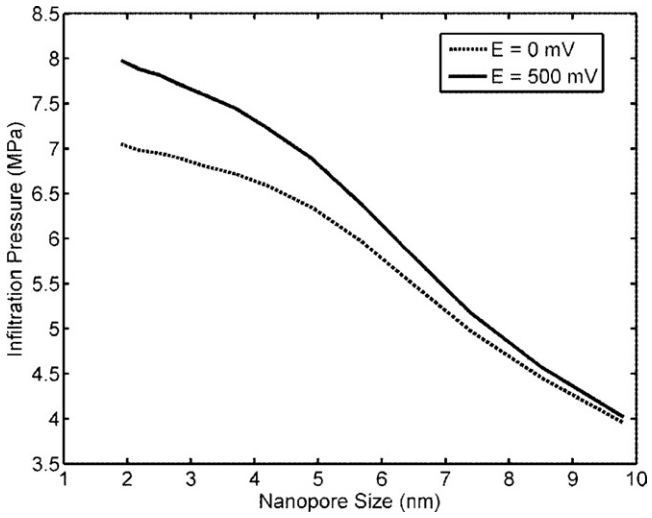

Fig. 3. The infiltration pressure as a function of the nanopore size.

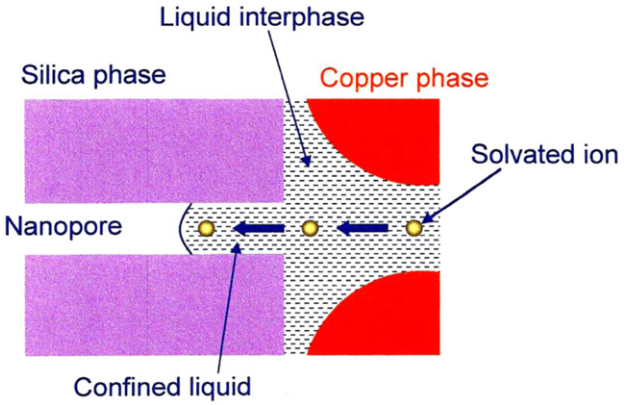

Fig. 4. Schematic of the surface charges at a nanopore opening.

Therefore, without any size effect, the wettability change should be comparable with that on a large electrode coated by a thin glass plate; the required voltage for detectable surface tension changes should be higher than tens of volts.

Fig. 2 indicates that, when the external voltage is applied, the measured ion transport pressure varies significantly. It is remarkable that the pressure increases. Moreover, the pressure increase is quite non-uniform over the infiltration plateau. The pressure change happens when the applied voltage is only 500 mV. At the beginning of infiltration, the pressure difference is small. As the liquid infiltration volume increases, the pressure difference rises monotonically to about 1 MPa. By using the nanopore size distribution data obtained in the BET measurement and a Washburn-type analysis [12], the accumulated pore volume can be related to the pore size, d, as shown in Fig. 3. Clearly, the pressure difference is more pronounced when the nanopore size is small. When the nanopore size is larger than 8 nm, the effect of voltage becomes trivial.

These phenomena are significantly different from the electrowetting of aqueous solutions on thiol-modified gold electrodes [28], and cannot be explained by the conventional theory. First, the applied voltage, E, is low. Since E is only 500 mV, it should not affect the liquid motion across the silica layer, which is at least a few μm thick. The observable effective interfacial tension change with such a low voltage usually happens at the surface of a conductive material, while the copper particles are solid and cannot affect the sorption isotherm curve. Second, the pressure increases with E. As discussed previously, if the pressure change is caused by the interfacial tension variation, it should decrease. Third, the pressure change is dependent on the nanopore size. In a relatively large pore, the pressure is insensitive to the voltage, which is consistent with the conventional theory. In a relatively small nanopore, the infiltration pressure increases by about 15%.

The measured infiltration pressure change may be attributed to the unique structure of nanopore opening and the large surface-to-volume ratio. At the opening of a large pore, as the liquid enters it, most of liquid molecules and ions are in the interior, far away from the outer surface of the porous particle. As depicted in Fig. 4, at the opening of a small nanopore, most of water molecules and solvated ions are exposed to the solid wall. If there is no external voltage, the influence of the pore opening is determined by the potential functions of solid atoms, water molecules, and solvated ions. There are two competitive intermolecular forces: solid–liquid adhesive and liquid–liquid cohesive interactions. If the cohesive interaction effect is stronger than the adhesive effect, the liquid is nonwetting to the solid, otherwise, it would be wetting [29]. With the external electric field, these effects still exist, while a new factor, the surface polarity, comes in. As the potential of the copper phase is higher than the potential of the liquid phase, an electric field is established normal to the outer surface of the HMS particle. While it promotes the motion of oppositely charged ions, an energy barrier to the like-charged ions is built up. The infiltration pressure is around a few MPa, insufficient to form a monopolar phase; that is, the cations and anions in the nanopore must be balanced. Hence, the higher resistance dominates the overall system behavior, and, consequently, the required pressure tends to increase.

The variation in infiltration pressure may also be related to the electro-viscosity effect. Some experiments on capillary filling of nanochannels have observed lower than expected filling rates [30,31]. Churaev et al. [32] found that the viscosity of water in glass capillaries of 80 nm diameter is approximately 40% elevated, and this elevation decreases rapidly with increasing channel size. Similarly, Tas et al. [31] found that the elevation of the apparent viscosity amounts up to $24 \pm 11\%$ for demineralized water in equilibrium with air in nanochannels. Mortensen and Kristensen [30] worked out the electro-viscous correction, including the Debye-layer correction, to the hydraulic resistance by using theoretical methods. However, in the present work, the loading rate is quasi-static and, therefore, the viscosity effect should be secondary.

It is clear that the above discussions do not provide a definitive answer for the mechanisms of the liquid infiltration under the influence of external electric field. Computer simulations need to be performed to examine the details of the solid–liquid interaction processes.

4. Concluding remarks

We report an experimental result that, when HMS is mixed with copper microparticles, the effective infiltration pressure of an electrolyte solution is sensitive to the external electric field. With a voltage of 500 mV, in the smallest nanopores the infiltration pressure increases by nearly 15%, while in the largest nanopores the pressure variation is negligible. These phenomena may be related to the effect of surface polarization amplified by the large surface area, and/or the electro-viscosity effect.

Acknowledgement

This work was supported by the National Science Foundation under Grant No. ECCS-1028010.

References

[1] N.A. Mortensen, L.H. Olesen, F. Okkels, H. Bruus, Nanoscale Microscale Thermophys. Eng. 11 (2007) 57–69.
[2] D.I. Dimitrov, A. Milchev, K. Binder, Phys. Rev. Lett. 99 (2007) 054501–054504.
[3] B.Y. Cao, J. Sun, M. Chen, Z.Y. Guo, Int. J. Mol. Sci. 10 (2009) 4638–4706.
[4] D. Nattua, Y. Gogotsi, Microfluid. Nanofluid. 5 (2008) 289–305.
[5] J.O.M. Bockris, S.U.M. Khan, Surface Electrochemistry, Springer, 1993.
[6] J. Zhao, P.J. Culligan, Y. Qiao, Q. Zhou, Y. Li, M. Tak, T. Park, X.J. Chen, Phys.: Condens. Matter 22 (2010) 315301.
[7] L. Liu, X. Chen, W. Lu, A. Han, Y. Qiao, Phys. Rev. Lett. 102 (2009), 184501.1–4.
[8] Y. Qiao, L. Liu, X. Chen, Nano Lett. 9 (2009) 984.
[9] H. Daiguji, Chem. Soc. Rev. 39 (2010) 901–911.
[10] G. Hummer, J.C. Rasaiah, J.P. Noworyta, Nature 414 (2001) 188–190.
[11] X. Chen, G. Cao, A. Han, V.K. Punyamurtula, L. Liu, P.J. Culligan, T. Kim, Y. Qiao, Nano Lett. 8 (2008) 2988–2992.
[12] A. Han, W. Lu, V.K. Punyamurtula, X. Chen, F.B. Surani, T. Kim, Y. Qiao, J. Appl. Phys. 104 (2008), 124908.1–4.
[13] W. Schmickler, E. Santos, Interfacial Electrochemistry, Springer, 2010.
[14] L. Liu, Y. Qiao, X. Chen, Appl. Phys. Lett. 92 (2008), 101927.1–3.
[15] T. Kim, W. Lu, A. Han, V.K. Punyamurtula, X. Chen, Y. Qiao, Appl. Phys. Lett. 94 (2009), 013105.1–3.
[16] W. Lu, T. Kim, A. Han, X. Chen, Y. Qiao, Langmuir 25 (2009) 9463–9466.
[17] Y. Qiao, V.K. Punyamurtula, A. Han, H. Lim, J. Power Sources 183 (2008) 403–405.
[18] A. Han, V.K. Punyamurtula, W. Lu, Y. Qiao, J. Appl. Phys. 103 (2008), 084318. 1–5.
[19] M.H. Lim, A. Stein, Chem. Mater. 11 (1999) 3285.
[20] Y. Qiao, G. Cao, X. Chen, J. Am. Chem. Soc. 129 (2007) 2355–2359.
[21] G.X. Cao, Y. Qiao, Q.L. Zhou, X. Chen, Mol. Simul. 34 (2008) 1267–1274.
[22] A. Han, X. Kong, Y. Qiao, J. Appl. Phys. 100 (2006), 014308.1–3.
[23] M.P. Soriaga, Electrochemical Surface Science, Am. Chem. Soc., 1988.
[24] J. Berthier, Microdrops and Digital Microfluidics, William Andrew, 2008.
[25] J.A.M. Sondag-Huethorst, L.G.J. Fokkink, Langmuir 11 (1995) 2237–2241.
[26] J.A.M. Sondag-Huethorst, L.G.J. Fokkink, Langmuir 8 (1992) 2560–2566.
[27] J. Sondag-Huethorst, L. Fokkink, J. Electroanal. Chem. 367 (1994) 49–57.
[28] M. Vallet, B. Berge, Polymer 37 (12) (1996) 2465–2470.
[29] M. Radiom, W.K. Chan, C. Yang, Microfluid. Nanofluid. 9 (2010) 65–75.
[30] N.A. Mortensen, A. Kristensen, Appl. Phys. Lett. 92 (2008) 063110.
[31] N.R. Tas, J. Haneveld, H.V. Jansen, M. Elwenspoek, A. van den Berg, Appl. Phys. Lett. 85 (15) (2004) 3274–3276.
[32] N.V. Churaev, V.D. Sobolev, Z.M. Zorin, Special Discussion on Thin Liquid Films and Boundary Layers, Academic, New York, 1971, pp. 213–220.